On finite-difference solutions in elasticity

ON FINITE-DIFFERENCE SOLUTIONS IN ELASTICITY

by
Robert Edward Fangmann

A Thesis Submitted to the Faculty of the

DEPARTMENT OF CIVIL ENGINEERING

In Partial Fulfillment of the Requirements
For the Degree of

MASTER OF SCIENCE

In the Graduate College

THE UNIVERSITY OF ARIZONA

1 9 6 7

STATEMENT BY AUTHOR

This thesis has been submitted in partial fulfillment of requirements for an advanced degree at the University of Arizona and is deposited in the University Library to be made available to borrowers under rules of the Library.

Brief quotations from this thesis are allowable without special permission, provided that accurate acknowledgment of source is made. Requests for permission for extended quotation from or reproduction of this manuscript in whole or in part may be granted by the head of the major department or the Dean of the Graduate College when in his judgment the proposed use of the material is in the interests of scholarship. In all other instances, however, permission must be obtained from the author.

SIGNED: Robert E. Fangmeier

APPROVAL BY THESIS DIRECTOR

This thesis has been approved on the date shown below:

Richmond C. Neff — 29 June 67

RICHMOND C. NEFF
Professor of Civil Engineering

Date

ACKNOWLEDGMENTS

The author wishes to express his sincere thanks to his major advisor, Dr. Richmond C. Neff, for his encouragement, guidance, and technical assistance during the preparation of this thesis.

The author also wishes to express his thanks to his wife, Bonnie, for her assistance in preparing his manuscript.

TABLE OF CONTENTS

TABLE OF CONTENTS--Continued

LIST OF ILLUSTRATIONS

LIST OF TABLES

LIST OF SYMBOLS

∇^4	Biharmonic operator.
δ_{ij}	Kronecker Delta.
E	Young's Modulus.
e_{ij}	strain tensor.
F	body force.
h	mesh spacing.
K	dominant eigenvalue of the iteration matrix.
L	length of the edge of the plate.
P	applied load.
s	Poisson's Ratio.
T_{ij}	stress tensor.
μ, λ	Lame's constants.
U	Airy's Stress Function.
u	horizontal displacement or displacement in the x_1 direction.
v	vertical displacement or displacement in the x_2 direction.
w_i	displacement vector.

ABSTRACT

This thesis demonstrates the feasibility of solving a mixed boundary-value problem in plane elasticity using a finite-difference form of Navier's Equations. Various grid spacings are used in the solution, with the result that the best grid system of those used is composed of a combination of mesh sizes. The finite-difference equations are solved by the method of iteration, with a scheme to accelerate the convergence. The acceleration scheme is found to make remarkable savings in computer time.

CHAPTER I

INTRODUCTION

Elasticity is the study of the response of an elastic material under various loads. An elastic material is one which deforms under load but returns to its original shape when the load is removed. Many solid materials exhibit elastic behavior over some range of loading.

In developing a mathematical theory of elasticity, elastic materials are usually assumed to be homogeneous and isotropic. These have been shown to be good assumptions. As Sokolnikoff (1956, p. 65) mentions,

> Most structural materials are formed of crystalline substances, and hence very small portions of such materials cannot be regarded as being isotropic. Nevertheless, the assumption of isotropy and homogeneity, when applied to an entire body, often does not lead to serious discrepancies between the experimental and theoretical results. The reason for this agreement lies in the fact that the dimensions of most crystals are so small in comparison with the dimensions of the body and they are so chaotically distributed that, in the large, the substance behaves as though it were isotropic.

Another assumption which is commonly made in elasticity is linearity, both geometric and material. The assumption of geometric linearity is satisfied if the derivatives of the displacements in the material are small enough to neglect products of these terms in comparison to

the terms themselves. Material linearity is satisfied if the material has a linear relationship between stress and strain in the elastic range. This has also been shown to be a good assumption for many engineering materials.

The system of governing equations in elasticity includes the equations of equilibrium, the stress-strain equations, and the compatibility equations. Also, equilibrium conditions must be satisfied at the boundary. This gives rise to boundary conditions which must be met.

Boundary conditions may be in terms of surface tractions or displacements. Both Boresi (1965) and Sokolnikoff (1956) list two fundamental types of boundary-value problems of elasticity. As presented by Sokolnikoff (1956, p. 73) these are:

> Problem 1. Determine the distribution of stress and the displacements in the interior of and elastic body in equilibrium when the body forces are prescribed and the distribution of the forces acting on the surface of the body is known.
>
> Problem 2. Determine the distribution of stress and the displacements in the interior of an elastic body in equilibrium when the body forces are prescribed and the displacements of the points on the surface of the body are prescribed functions.

There is a third type, usually called the Mixed Boundary-Value Problem, which is a combination of these two: Determine the distribution of stress and displacements in the interior of an elastic body in equilibrium when the body forces are prescribed and the displacements of the

points on part of the surface of the body are prescribed function and the distribution of the forces acting on the remaining part of the surface of the body is known. This mixed boundary-value problem is the one with which this thesis is concerned.

Frequently it is difficult to express the boundary conditions in a convenient mathematical form. Often it is possible to modify the boundary conditions slightly and obtain an approximate solution. The modifications must be in accordance with Saint Venant's Principle which, as stated by Sokolnikoff (1956, p. 90), is,

> If some distribution of forces acting on a portion of the surface of a body is replaced by a different distribution of forces acting on the same portion of the body, then the effects of the two different distributions on the parts of the body sufficiently far removed from the region of application of the forces are essentially the same, provided that the two distributions of forces are statically equivalent.

This principle is of great practical importance. As an example, a point load is difficult to express in any convenient mathematical form, whereas it is relatively simple to treat it as a distributed load over a small area of the boundary.

There is a Uniqueness Theorem associated with linear elasticity which states that there is only one solution with satisfies the governing equations -- equilib-

rium, compatibility, and stress-strain -- and the boundary conditions. A proof of this is presented by Sokolnikoff (1956, pp. 86-88).

There are three methods of obtaining analytic solutions to the above boundary-value problems. The Direct Method is to solve the governing differential equations directly while satisfying all the boundary conditions. The Inverse Method involves finding a problem to fit a proposed solution. The Semi-inverse Method consists in making some assumptions about part of the solution while leaving sufficient generality in the solution to satisfy the governing equations and the boundary conditions. If a solution is obtained, according to the Uniqueness Theorem, it is the only solution.

The work involved in the Direct Method is very often prohibitive beyond a few almost trivial problems. The Inverse Method is almost useless if there is a specific problem to be solved. The Semi-inverse Method, therefore, is the one most often employed. In most problems, simplifying assumptions can be made as the result of symmetry or of the experience of the investigator in solving similar problems. Such freedom is possible due to the existence of the Uniqueness Theorem.

In plane elasticity, the Airy Stress Function may be employed so that the problem is reduced to a solution of the biharmonic equation $\nabla^4 U = 0$, and where U is Airy's Stress Function. Of course, boundary conditions must also be satisfied. Again the Direct, Inverse, or Semi-inverse Method may be used.

The theory of linear elasticity and the different methods of solution, which are summarized above, have existed for one hundred years. However, due to the complicated nature of elasticity problems, only the simplest problems have been solved in closed form. Recently the computer has made it possible to apply numerical methods to the solution of the differential equations of elasticity. Griffin and Varga (1963) and Allen (1954) have shown that this method yields a good approximate solution.

Numerical analysis is most often applied to the biharmonic equation. As shown in Salvadori and Baron (1961) and Allen (1954), this method yields a system of linear algebraic equations which can be solved for values of the stress function at a number of points in the body and on the boundary. From these values, stresses and displacements may be calculated at discrete points in the body and on the boundary. Griffin and Varga (1963) have demonstrated the usefulness and flexibility of the method. However, in order to solve the biharmonic equation for the stress

function, it is necessary to express the boundary conditions in terms of the stress function. Because there is only an indirect relationship between the stress function and displacements, it is difficult, if not impossible, to apply this method to the second or to the mixed type of boundary-value problem.

Numerical analysis can also be applied to some other form of the governing equations. This thesis is concerned with the numerical solution of Navier's Equations with mixed boundary conditions. Navier's Equations relate displacements and body forces and are derived using the equilibrium equations, the stress-strain equations, and the strain-displacement relations. Navier's Equations yield displacements from which the stresses can be calculated.

Applying numerical methods to Navier's Equations yields a set of linear algebraic equations with displacements as unknowns. To solve this set of equations, an iterative method with an acceleration scheme due to Faddeeva (1959) is used. Faddeeva's acceleration scheme involves obtaining the dominant eigenvalue of the iteration matrix and using it to accelerate the convergence of iteration.

The photoelastic method of obtaining a solution to the same problem is used as a check on the accuracy of the approximate numerical solution. The photoelastic method is an experimental method which is subject only to experimental errors in manufacture and loading of the model, in measuring of data, and in defects in the optical system.

CHAPTER II

DERIVATION OF THE WORKING EQUATIONS

Derivation of Navier's Equations

The governing equations of elasticity as listed in Sokolnikoff (1956, p. 71) are:

the equations of equilibrium

$$T_{ij,j} + F_i = 0 \qquad (i,j = 1,2,3) \qquad (2.1)$$

the stress-strain relations

$$T_{ij} = \lambda \delta_{ij} e_{kk} + 2\mu e_{ij} \qquad (k = 1,2,3) \qquad (2.2)$$

and the compatibility equations

$$e_{ij,k\ell} + e_{k\ell,ij} - e_{j\ell,ik} = 0 \qquad (\ell = 1,2,3) \qquad (2.3)$$

where

T_{ij} = stress tensor

F = body forces

δ_{ij} = the Kronecker delta

e_{ij} = strain tensor

μ and λ = Lame's constants.

subscripts are in accordance with standard tensor notation where a comma used as a subscript denotes differentation.

Differentiating the stress-strain relations, substituting this into the equations of equilibrium, and using the strain-displacement relations

$$e_{ij} = 1/2(w_{i,j} + w_{j,i}) \tag{2.4}$$

yield

$$0 = \mu w_{i,jj} + (\lambda + \mu)w_{j,ji} + F_i \tag{2.5}$$

where w_i = displacement vector.

Equations (2.5) are Navier's Equations in three dimensions.

Navier's Equations for Plane Stress

For plane stress, we take $T_{13} = T_{23} = T_{33} = F_3 = 0$. Consider the stress-strain equation for T_{33}.

$$T_{33} = 0 = 2\mu w_{3,3} + \lambda(w_{1,1} + w_{2,2} + w_{3,3}) \tag{2.6}$$

so $$w_{3,3} = -\frac{\lambda}{\lambda + 2\mu}(w_{1,1} + w_{2,2}) \tag{2.7}$$

and $$w_{3,3} = -\frac{\lambda}{\lambda + 2\mu}(w_{\alpha,\alpha}) \qquad (\alpha = 1,2) \tag{2.8}$$

but $$w_{k,k} = w_{\alpha,\alpha} + w_{3,3} \tag{2.9}$$

Substituting for $w_{3,3}$ from Equation (2.8) yields

$$w_{k,k} = \frac{2\mu}{\lambda + 2\mu} w_{\alpha,\alpha} \tag{2.10}$$

Now consider the stress-strain equations for plane stress.

$$T_{\alpha\beta} = \mu(w_{\alpha,\beta} + w_{\beta,\alpha}) + \lambda\delta_{\alpha\beta}w_{k,k} \quad (\beta = 1,2) \quad (2.11)$$

Substituting for $w_{k,k}$ from Equation (2.10) yields

$$T_{\alpha\beta} = \mu(w_{\alpha,\beta} + w_{\beta,\alpha}) + \frac{2\mu\lambda}{\lambda + 2\mu}\delta_{\alpha\beta}w_{\gamma,\gamma} \quad (\gamma = 1,2) \quad (2.12)$$

The equilibrium equations for plane stress are

$$T_{\alpha\beta,\beta} + F_{\alpha} = 0 \quad (2.13)$$

Differentiating Equations (2.12) with respect to β yields

$$T_{\alpha\beta,\beta} = \mu(w_{\alpha,\beta\beta} + w_{\beta,\alpha\beta}) + \frac{2\mu\lambda}{\lambda + 2\mu}\delta_{\alpha\beta}w_{\gamma,\gamma\beta} \quad (2.14)$$

Substituting this into the equilibrium equations yields

$$0 = \mu(w_{\alpha,\beta\beta} + w_{\beta,\alpha\beta}) + \frac{2\mu\lambda}{\lambda + 2\mu}\delta_{\alpha\beta}w_{\gamma,\gamma\beta} + F_{\alpha} \quad (2.15)$$

or $$0 = \mu w_{\alpha,\beta\beta} + \frac{\mu(2\mu + 3\lambda)}{\lambda + 2\mu}w_{\beta,\beta\alpha} + F_{\alpha} \quad (2.16)$$

Let $C = \dfrac{2\mu + 3\lambda}{\lambda + 2\mu}$

Then $$0 = w_{\alpha,\beta\beta} + Cw_{\beta,\beta\alpha} + \frac{F_{\alpha}}{\mu} \quad (2.17)$$

Equations (2.17) are Navier's Equations for plane stress.

Navier's Equations for Plane Strain

For plane strain, $e_{31} = e_{32} = e_{33} = w_{i,3} = 0$. Expanding Navier's Equations in three dimensions and imposing the restrictions for plane strain yields

$$0 = \mu w_{\alpha,\beta\beta} + (\lambda + \mu)\, w_{\beta,\beta\alpha} + F_\alpha \qquad (2.18)$$

or $$0 = w_{\alpha,\beta\beta} + \frac{(\lambda + \mu)\, w_{\beta,\beta\alpha}}{\mu} + \frac{F_\alpha}{\mu} \qquad (2.19)$$

Let $C' = \frac{\lambda + \mu}{\mu}$

Then $$0 = w_{\alpha,\beta\beta} + C' w_{\beta,\beta\alpha} + \frac{F_\alpha}{\mu} \qquad (2.20)$$

Equations (2.20) are Navier's Equations for plane strain.

Summarizing, Navier's Equations for two dimensions are

$$0 = w_{\alpha,\beta\beta} + C w_{\beta,\beta\alpha} + \frac{F_\alpha}{\mu} \quad \text{for plane stress} \qquad (2.21)$$

and $$0 = w_{\alpha,\beta\beta} + C' w_{\beta,\beta\alpha} + \frac{F_\alpha}{\mu} \quad \text{for plane strain} \qquad (2.22)$$

Since $E = \frac{\mu(3\lambda + 2\mu)}{\lambda + \mu}$ and $s = \frac{\lambda}{2\lambda + 2\mu}$,

$C = \frac{1 + s}{1 - s}$ and $C' = \frac{1}{1 - 2s}$ where

E = Young's Modulus and s = Poisson's Ratio. Notice that the two constants which express the material properties are functions of Poisson's Ratio only.

For the problem proposed in Chapter III, the plane stress form of Navier's Equations is used.

Boundary Conditions

The boundary conditions are of two types. First, where displacements are specified, there is no difficulty since Navier's Equations are in terms of displacements. Second, where tractions are specified, the stress-strain equations for plane stress are used to express the tractions in terms of derivatives of displacements.

Summary

In expanded form, Navier's Equations for plane stress, Equations (2.21) are

$$0 = (1 + C)\, u_{,11} + C v_{,21} + u_{,22} + \frac{F_1}{\mu}$$

and $$0 = (1 + C)\, v_{,22} + C u_{,12} + v_{,11} + \frac{F_2}{\mu} \qquad (2.23)$$

where u is the displacement in the x_1 direction

and v is the displacement in the x_2 direction.

In expanded form, Equations (2.12) become:

$$T_{11} = 2\mu\, u_{,1} + \frac{2\mu\lambda}{\lambda + 2\mu} (u_{,1} + v_{,2})$$

$$T_{22} = 2\mu\, v_{,2} + \frac{\mu\lambda}{\lambda + 2\mu} (u_{,1} + v_{,2})$$

$$T_{12} = \mu(u_{,2} + v_{,1}) \qquad (2.24)$$

where

T_{11} = normal stress in the x_1 direction

T_{22} = normal stress in the x_2 direction

T_{12} = shear stress.

Equations (2.24) are used to obtain the boundary conditions at boundary points at which surface tractions are prescribed, and also to obtain the stresses at interior points when the displacements have been determined.

CHAPTER III

FINITE-DIFFERENCE REPRESENTATION OF THE WORKING EQUATIONS

The specific problem to be solved is that of finding displacements and stresses for the flat plate supported and loaded as shown in Figure 1.

As is usual in finite-difference solutions, a square mesh is superimposed on the figure, and displacements and stresses are evaluated at the junctions of the mesh, called node points. According to Salvadori and Baron (1961), the error involved in this approximate solution is proportional to some power of h, where h is the mesh spacing. To attack this problem numerically, Navier's Equations and the boundary conditions must be expressed as finite-difference equations.

From Salvadori and Baron (1961), derivatives may be expressed in terms of central differences with an error of the order of h^2.

$$u_{i,1} = \frac{1}{2h} (u_r - u_\ell)$$

$$u_{i,11} = \frac{1}{h^2} (u_r - 2u_i + u_\ell)$$

$$u_{i,2} = \frac{1}{2h} (u_a - u_b)$$

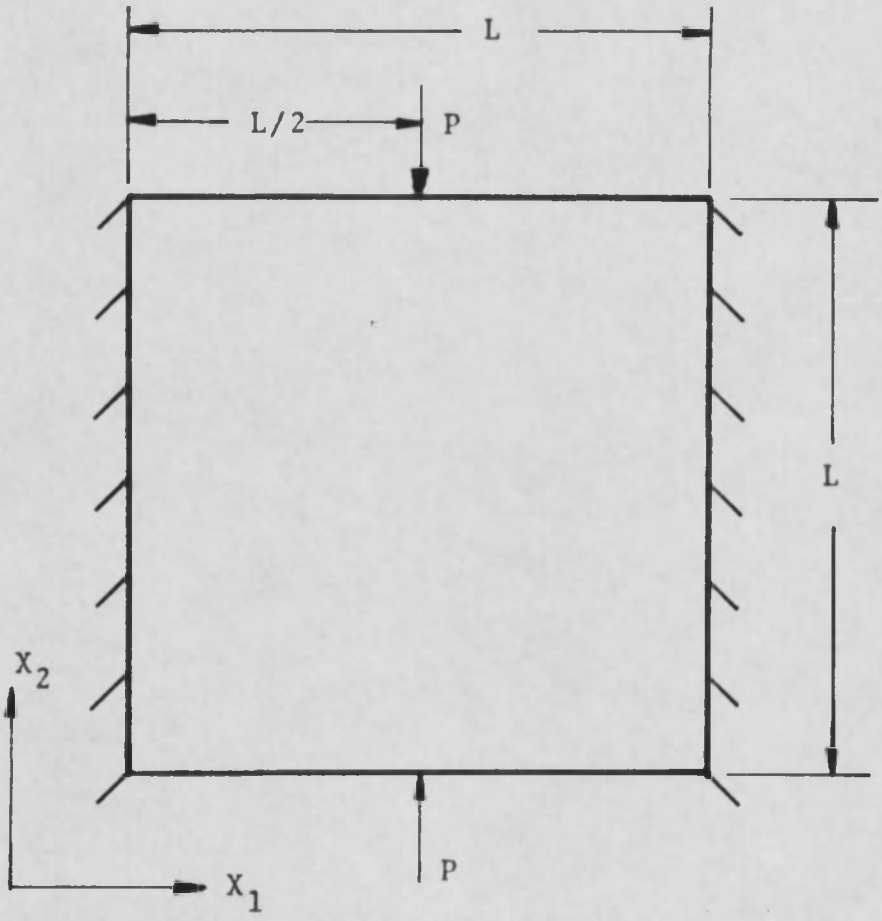

Figure 1

Clamped Plate with Concentrated Loads

$$u_{i,22} = \frac{1}{h^2} (u_a - 2u_i + u_b)$$

$$v_{i,1} = \frac{1}{2h} (v_r - v_\ell)$$

$$v_{i,11} = \frac{1}{h^2} (v_r - 2v_i + v_\ell)$$

$$v_{i,2} = \frac{1}{2h} (v_a - v_b)$$

$$v_{i,22} = \frac{1}{h^2} (v_a - 2v_i + v_b)$$

$$u_{i,12} = \frac{1}{4h^2} (u_{\ell b} - u_{rb} - u_{\ell a} + u_{ra})$$

$$v_{i,21} = \frac{1}{4h^2} (v_{b\ell} - v_{a\ell} - v_{br} + v_{ar}) \qquad (3.1)$$

The subscripts r, ℓ, a, and b designate displacements at points which are either to the right, or left, above, or below the i^{th} point where the derivative is being evaluated, as shown in Figure 2. The parameter h is the mesh spacing.

Navier's Equations

Applying Equations (3.1) to Navier's Equations, Equations (2.23), for plane stress yields

$$0 = (1 + C)(u_r - 2u_i + u_\ell) + \frac{C}{4}(v_{ar} - v_{br} - v_{a\ell} + v_{b\ell}) + u_a - 2u_i + u_b + \frac{h^2 F_1}{\mu}$$

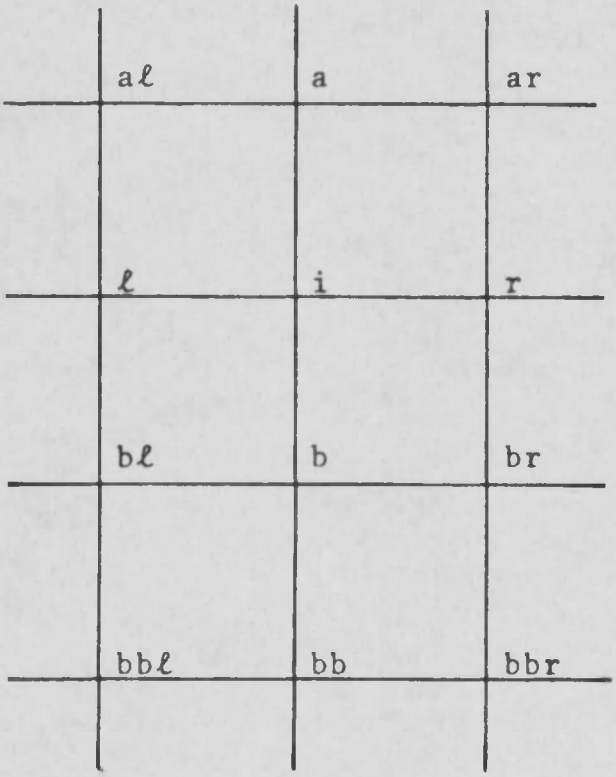

Figure 2

Indexing Procedure for Nodal Points

and $$0 = (1 + C)(v_a - 2v_i + v_b) + \frac{C}{4}(u_{ar} - u_{br} - u_{a\ell} + u_{b\ell}) + v_r - 2v_i + v_\ell + \frac{h^2 F_2}{\mu} \qquad (3.2)$$

Boundary Conditions

Expressing the boundary conditions, Equations (2.24), as finite-difference equations yields

$$T_{22} = \frac{2\mu\lambda}{\lambda + 2\mu}\left(\frac{1}{2h}\right)(u_r - u_\ell) + \frac{4\mu^2 + 4\mu\lambda}{2h(\lambda + 2\mu)}(v_a - v_b)$$

and $$T_{12} = \left(\frac{1}{2h}\right)\mu(u_a - u_b + v_r - v_\ell) \qquad (3.3)$$

The equation for T_{11} is not included since it does not enter into the proposed problem.

For the proposed problem, the shear stress is zero on the upper and lower edges. So

$$T_{12} = 0 = \left(\frac{1}{2h}\right)\mu(u_a - u_b + v_r - v_\ell)$$

or $$0 = u_a - u_b + v_r - v_\ell \qquad (3.4)$$

Where the normal stress is zero on the boundary, the equation for T_{22} becomes

$$0 = \lambda(u_r - u_\ell) + 2(\mu + \lambda)(v_a - v_b) \qquad (3.5)$$

Where the load, P, is applied, Saint Venant's Principle is invoked. The concentrated load, P, is replaced by the statically equivalent distributed load, $\frac{P}{h}$, which is applied over a length, h, of the boundary. The distributed load is, of course, centered about the point where the concentrated load was originally applied, so that the resultant of the distributed load is equal to the applied load. The boundary condition equation expressing the normal stress at this point on the upper edge becomes

$$-P\left(\frac{\lambda + 2\mu}{\mu}\right) = \lambda(u_r - u_\ell) + 2(\mu + \lambda)(v_a - v_b) \tag{3.6}$$

If the boundary conditions are all in terms of displacements, only interior nodal points are needed. This easily yields a solution. If all boundary conditions are in terms of tractions, all interior and boundary mesh points are required. This necessitates the use of exterior mesh points, thus introducing more unknowns. But boundary conditions provide the necessary extra equations. However, if the problem has mixed boundary conditions, care must be taken to use all the boundary conditions and still balance the number of unknowns and equations.

Transition Points

In the plate shown in Figure 1, and in general in any mixed boundary value problem of this type, Navier's Equations must be applied to every interior nodal point and to any boundary point where displacements are not specified. When Navier's Equations are appled to these boundary points, exterior mesh points will be introduced as unknowns. But the tractions specified at these points will provide extra equations to balance these exterior unknowns. The problem occurs in applying Navier's Equations to a transition point. A transition point is any boundary point where tractions are specified and a neighboring boundary point has its displacement specified. In order to apply Navier's Equations to such a point, the displacements of the nodes exterior to the neighboring nodes are introduced. But since the neighboring nodes have their displacements specified, there are no additional equations to balance this additional exterior unknown. This difficulty is remedied by expressing the mixed derivatives in Navier's Equations in terms of inward differences before they are applied to a transition boundary point.

For the problem shown in Figure 1, due to symmetry conditions, only one quarter of the plate must be solved. For the purpose of discussion, consider the upper right quarter of the plate shown in Figure 3 with the coarsest possible mesh superimposed upon it.

The transition point for this problem is the point marked with an X in Figure 3. For this point, the finite-difference equations take the form

$$0 = (1 + C)(u_r - 2u_i + u_\ell) + \frac{C}{4}(v_{rbb} - v_{\ell bb} - 4v_{rb} + 4v_{\ell b} + 3v_r - 3v_\ell) + u_a - 2u_i - u_b + \frac{h^2 F_1}{\mu}$$

and

$$0 = (1 + C)(v_a - 2v_i + v_b) + \frac{C}{4}(u_{rbb} - u_{\ell bb} - 4u_{rb} + 4u_{\ell b} + 3u_r - 3u_\ell) + v_r - 2v_i + v_\ell + \frac{h^2 F_2}{\mu} \qquad (3.7)$$

The mixed derivatives have been expressed in terms of inward differences which also have an h^2 error.

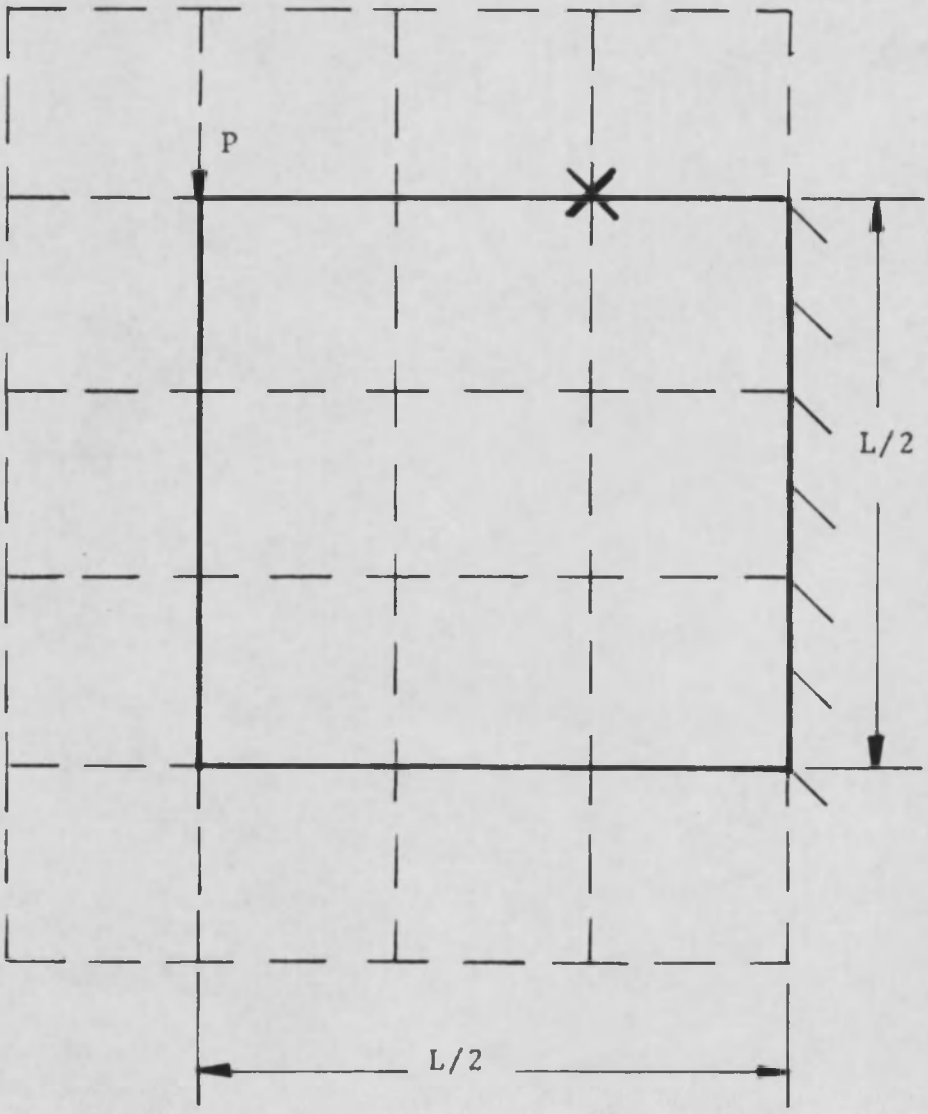

Figure 3

Coarse Mesh Superimposed on One

Quarter of the Clamped Plate

——— Edges of the quarter plate
— — Superimposed mesh lines

Summary

Summarizing, the finite-difference equations which are used to solve the flat plate problem are given below.

Navier's Equations, Equations (3.2), in terms of central differences, neglecting body forces are

$$2(2 + C)u_i = (1 + C)\,(u_r + u_\ell) + \frac{C}{4}\,(v_{ar} - v_{br} - v_{a\ell} + v_{b\ell}) + u_a + u_b$$

and

$$2(2 + C)v_i = (1 + C)\,(v_a + v_b) + \frac{C}{4}\,(u_{ar} - u_{a\ell} - u_{br} + u_{b\ell}) + v_r + v_\ell \qquad (3.8)$$

which are applied at all interior nodes and boundary nodes where tractions are specified except transition points.

Navier's Equations with mixed derivatives in terms of inward differences, Equations (3.7), neglecting body forces, are

$$2(2 + C)u_i = (1 + C)\,(u_r + u_\ell) + \frac{C}{4}\,(v_{bbr} - v_{bb\ell} - 4v_{br} + 4v_{b\ell} + 3v_r - 3v_\ell) + u_a + u_b$$

and

$$2(2 + C)v_i = (1 + C)\,(v_a + v_b) + \frac{C}{4}\,(u_{bbr} - u_{bb\ell} - 4u_{br} + 4u_{b\ell} + 3u_r - 3u_\ell) + v_r + v_\ell \qquad (3.9)$$

which are applied at transition node points.

Boundary Condition Equations are:

Equation (3.4)

$$u_i = u_{bb} + v_{b\ell} - v_{br} \tag{3.10}$$

which is applied at all exterior points where tractions are specified,

Equation (3.6)

$$v_i = v_{bb} - \frac{P\left(\frac{\lambda + 2\mu}{\mu}\right) + (u_{br} - u_{b\ell})}{2(\mu + \lambda)} \tag{3.11}$$

which is applied at the node exterior to the point where the load, P, acts,

and Equation (3.5)

$$v_i = v_{bb} - \lambda \frac{(u_{br} - u_{b\ell})}{2(\mu + \lambda)} \tag{3.12}$$

which is applied at all exterior nodes where tractions are specified, except where Equation (3.11) is applied.

The equations listed in the summary refer to the displacements of the i^{th} nodal point in terms of the displacements at neighboring nodal points. All these equations have an error of the order of h^2.

Stress-Strain Equations

The equations in the summary are the general working equations, and they yield displacements as results. To solve for the stresses at all nodal points in the plate, the stress-strain equations for plane stress must be expressed as finite-difference equations. The stresses at the i^{th} nodal point are:

$$T_{11} = \frac{4\mu(\mu + \lambda)}{2h(\lambda + 2\mu)} (u_r - u_\ell) + \frac{2\mu\lambda}{2h(\lambda + 2\mu)} (v_a - v_b)$$

$$T_{22} = \frac{4\mu(\mu + \lambda)}{2h(\lambda + 2\mu)} (v_a - v_b) + \frac{2\mu\lambda}{2h(\lambda + 2\mu)} (u_r - u_\ell)$$

and $$T_{12} = \frac{1}{2h} \mu(u_a - u_b + v_r - v_\ell) \qquad (3.13)$$

As before, the transition point requires the use of inward differences since the displacements of the node exterior to its adjacent point cannot be given in finite-difference form. The equations for the stresses at the transition point are:

$$T_{11} = \frac{4\mu(\mu + \lambda)}{2h(\lambda + 2\mu)} (u_{\ell\ell} - 4u_\ell + 3u_i)$$

$$+ \frac{2\mu\lambda}{2h(\lambda + 2\mu)} (v_{bb} - 4v_b + 3v_i)$$

$$T_{22} = \frac{4\mu(\mu + \lambda)}{2h(\lambda + 2\mu)} (v_{bb} - 4v_b + 3v_i)$$

$$+ \frac{2\mu\lambda}{2h(\lambda + 2\mu)} (u_{\ell\ell} - 4u_\ell + 3u_i)$$

and $$T_{12} = \frac{\mu}{2h} (u_{bb} - 4u_b + 3u_i + v_{\ell\ell} - 4v_\ell + 3v_i) \quad (3.14)$$

With displacements known, Equations (3.13) and (3.14) easily yield stresses.

Graded Mesh

The finite-difference equations listed above are derived using a square mesh, so the mesh size can be expressed in terms of one parameter, h, which is the mesh spacing. The solution obtained using those equations contains an error of the order of h^2.

One method of obtaining a better solution is to use a finer grid, that is, to reduce the value of h. But this causes an increase in the number of equations. This, in turn, increases computer time and expense.

Frequently in a problem of this type, a coarse mesh is satisfactory over a large portion of the plate, but a finer mesh is necessary over a critical section. In the proposed problem, the critical section occurs in the vicinity of the applied load.

An obvious solution is to superimpose a fine mesh over the critical region and a coarse mesh over the remainder of the plate. Thus, the error in the critical region is reduced while keeping the number of equations to a minimum. However, using a graded mesh increases the complexity of the problem.

Consider the coarse mesh shown in Figure 3, but with a finer mesh in the region of the applied load as shown in Figure 4.

The displacements at the points marked with an X are needed in order to evaluate the displacements at many of the nodes of the finer mesh. However, these points are not nodal points, and therefore their displacements at these points are found by averaging the values of the displacements at nodes nearby.

The displacements of the points, X, which are in the interior of the plate and are in the center of a mesh square are evaluated by averaging the displacements at the nodes on the corners of the square. For these displacements, the equations are

$$u_i = .25\ (u_{ar} + u_{a\ell} + u_{br} + u_{b\ell})$$

and $$v_i = .25\ (v_{ar} + v_{a\ell} + v_{br} + v_{b\ell}) \qquad (3.15)$$

The displacements of the points, X, which are on mesh lines, are evaluated by averaging the displacements at the two nearest nodes. If the point lies on a vertical mesh line, the equations for its displacements are

$$u_i = .5\ (u_a + u_b)$$

and $$v_i = .5\ (v_a + v_b) \qquad (3.16)$$

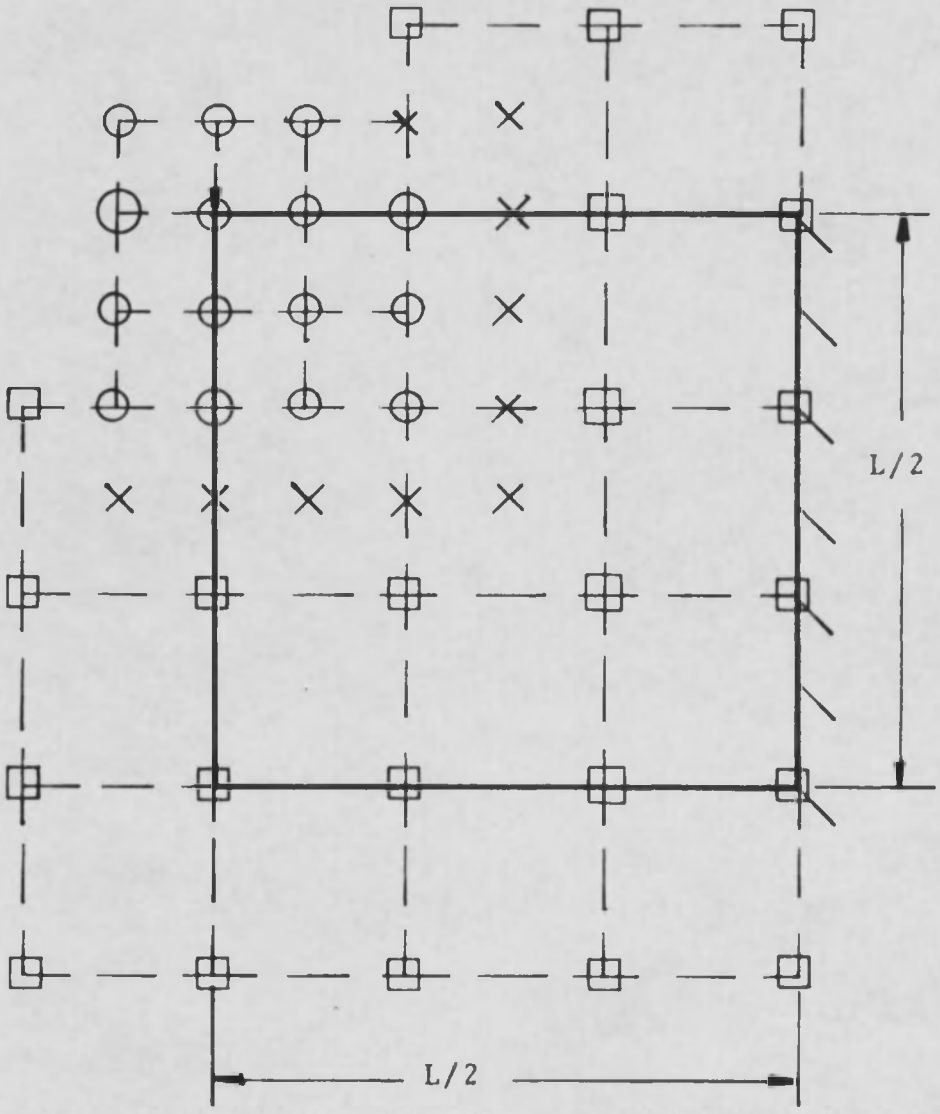

Figure 4

Graded Mesh Superimposed on One

Quarter of the Clamped Plate

——— Edges of the quarter plate
— — Superimposed mesh lines

If the point lies on a horizontal mesh line, the equations for its displacements are

$$u_i = .5\ (u_r + u_\ell)$$

and $$v_i = .5\ (v_r + v_\ell) \qquad (3.17)$$

For the point, X, exterior to the plate but not on a mesh line, the boundary-condition equations are used.

The displacements at the nodes marked with a circle, ○, are evaluated using the general working equations as if only the fine mesh were used for the entire plate. The displacements at the nodes marked with a square, □, are evaluated using the general working equations as if only the coarse mesh were used.

This averaging process is actually an application of Bessel's Formula for Interpolating to Halves (Scarborough 1958, p. 77) using only first differences. If the change were something other than halving the coarse mesh, a more general interpolation formula must be used.

CHAPTER IV

METHODS OF SOLUTION

Numerical Solution

There are many schemes which may be used to solve a system of linear algebraic equations such as the system generated by the finite-difference equations applied to this problem. Because of the large number of equations and the ready availability of the IBM 7072 digital computer, the Gauss - Seidel Method of Iteration was chosen as the method of solution. The equations in Chapter III were formulated for an iterative solution; that is, each equation expresses the displacement at a node in terms of displacements at neighboring nodes.

It is well known that the method of iteration often uses a relatively large amount of computer time. In an effort to minimize the computer time, a scheme to accelerate the convergence of the set of equations is used. This scheme is presented by Faddeeva (1959). It consists in extracting the dominant eigenvalue of the iteration matrix, and using this eigenvalue in an equation to extrapolate to new values of displacements in place of an iteration.

The two extrapolation equations are

$$u_i^{(n)} = u_i^{(n-2)} + \frac{u_i^{(n-1)} - u_i^{(n-2)}}{1 - K}$$

and $$v_i^{(n)} = v_i^{(n-2)} + \frac{v_i^{(n-1)} - v_i^{(n-2)}}{1 - K} \qquad (4.1)$$

where n designates the extrapolated value, n-1 designates the last iteration value, and n-2 designates the next to the last iteration value. K is the dominant eigenvalue.

The proposed problem was solved using the iteration method with Faddeeva's acceleration scheme for three different mesh sizes. First, a solution was obtained using a coarse mesh with $h=\frac{L}{6}$ as shown in Figure 3. The second and third solutions were obtained using a middle-sized mesh with $h=\frac{L}{12}$ and a fine mesh with $h=\frac{L}{24}$. The computer program used for the fine mesh is given in the Appendix.

As a comparison, the problem was also solved for the same three mesh sizes using the Gauss - Seidel Method of Iteration without Faddeeva's acceleration scheme.

Also, in order to determine the feasibility of varying the mesh size, solutions were obtained for the proposed problem using a coarse graded mesh of size $h=\frac{L}{6}$

with a mesh of size $h=\frac{L}{12}$ in the vicinity of the load as shown in Figure 4, and a fine graded mesh of size $h=\frac{L}{12}$ with a mesh of size $h=\frac{L}{24}$ in the vicinity of the load.

The convergence rates of the different solutions are listed in Table 1. The IBM 7072 lists total time used in one minute increments, so for the solutions which took two minutes or less, the number of iterations is a better measure of the difference in convergence rates. The most dramatic difference occurs in the comparison of the convergence rate of the fine mesh solution using Faddeeva's acceleration scheme with that of the fine mesh solution using only iteration.

From the results in Table 1, it can be stated that the solution of a system of linear algebraic equations will converge approximately twice as fast using Faddeeva's acceleration scheme as the same system without the acceleration scheme. This estimate is based on the relative convergence rates of only three systems of equations. More investigation is necessary before any authoritative statement regarding Faddeeva's acceleration scheme can be made. However, the results in Table 1 indicate that such an investigation could be very fruitful.

Table 1

Convergence Rates for Numerical Solutions

Mesh Size	Iteration with Acceleration		Iteration with Acceleration	
	Number of Iterations	Computer Time	Number of Iterations	Computer Time
Coarse	28	1 min.	67	1 min.
Middle-sized	108	1 min.	228	2 min.
Fine	367	8 min.	866	18 min.
Coarse Graded	62	1 min.		
Fine Graded	501	8 min.		

As stated previously, a numerical solution of Navier's Equations yields displacements. Using the finite-difference form of the stress-strain equations, vertical and horizontal normal stresses with the associated shear stresses were obtained. Through the Mohr's Circle relationships, maximum shear stress was obtained at all node points on the plate. A graphical comparison of the stresses with the photelastic solution is presented in Chapter V of the thesis.

Photoelastic Solution

Photoelasticity is a standard method employed in plane stress analysis (Jessop and Harris 1950, Lee 1950). In this thesis, the photoelastic method was used to determine the isochromatic lines, that is the lines of constant maximum shear stress in a model which is shaped, supported, and loaded in the same manner as the plate in the proposed problem.

Before the model can be tested, the model constant must be determined. This constant is a function of the thickness and the optical properties of the model material. The material used was CR-39 with a thickness of .25 inches. Using the standard beam method of calibration (Lee 1950, pp. 166-167), the model constant was found to be 175 psi. per fringe.

Figure 5 is a photograph of one quarter of the 3-inch by 3-inch photoelastic model with a vertical applied load of 405 pounds. The upper right corner is the point of application of the load, the lower right corner is the middle of the plate, and the left edge is clamped. The wide, dark curve in the upper right corner marks the edge of a local lens formed by relatively large displacements normal to the plate in the vicinity of the applied load. The oyster shell figure is the left of this lens is caused by a small crack in the material at that point. As the applied load was increased from 0 to 405 pounds, it was observed that the lens and the crack affected the fringe pattern only in their immediate vicinity. The dark spot on the left side of the lower edge is a point of zero maximum shear stress. The closest dark line to this zero point is the locus of points with maximum shear stress equal to 175 psi. Each succeeding dark line is the locus of points where the maximum shear stress is increased by 175 psi. over that of the previous line. So from the photograph, the distribution of maximum shear stress over the plate can be determined.

Although the photoelastic solution is used in this thesis as a check on the accuracy of the numerical solution, the maximum shear stresses obtained by the photoelastic method contain errors due to imperfections in the optical

Figure 5

Photograph of Photoelastic Model Showing Isochromatic Fringes for an Applied Load of 405 Pounds

system used, methods of machining and loading the model, and interpolation in reading the photograph. Considering all these causes, the total error in the photoelastic solution is estimated to be one-half of a fringe or approximately 88 psi.

CHAPTER V

RESULTS AND CONCLUSIONS

To compare the results of the numerical and photoelastic methods of solution, the maximum shear stress for both methods is shown in graphical form for an applied load of 405 pounds in Figure 6 and Figure 7.

Figure 6 is a graph of maximum shear stress versus position on the plate along a vertical line from the load point to the middle of the plate. Figure 7 is the same type of graph along a horizontal line from the middle of the plate to the clamped edge. Together these graphs display the variation of shear stress from a maximum to a minimum value on the plate.

Accuracy of Numerical Solutions

The finite-difference representations of the governing differential equations contain an error proportional to the square of the mesh spacing and the gradient of the displacements in the plate. For the numerical solutions with constant mesh size, the least error would be expected in those regions of the plate where the displacements varied the least. However, considering the round-off errors and the convergence test in the computational

Figure 6

Maximum Shear Stress as a Function of Position from the Load Point to the Middle of the Plate

Curve 1 -- the coarse mesh solution
Curve 2 -- the coarse graded mesh solution
Curve 3 -- the middle-sized mesh solution
Curve 4 -- the fine graded mesh solution
Curve 5 -- the fine mesh solution
Curve 6 -- the photoelastic solution

The photoelastic solution is shown in its entirety as well as the photograph could be read. The curves of the numerical solutions are discontinued for clarity. The portions of the curves which are omitted all lie within 60 psi. of the photoelastic solution. On the abscissa, the zero point is the point of application of the load and L/2 is the middle of the plate.

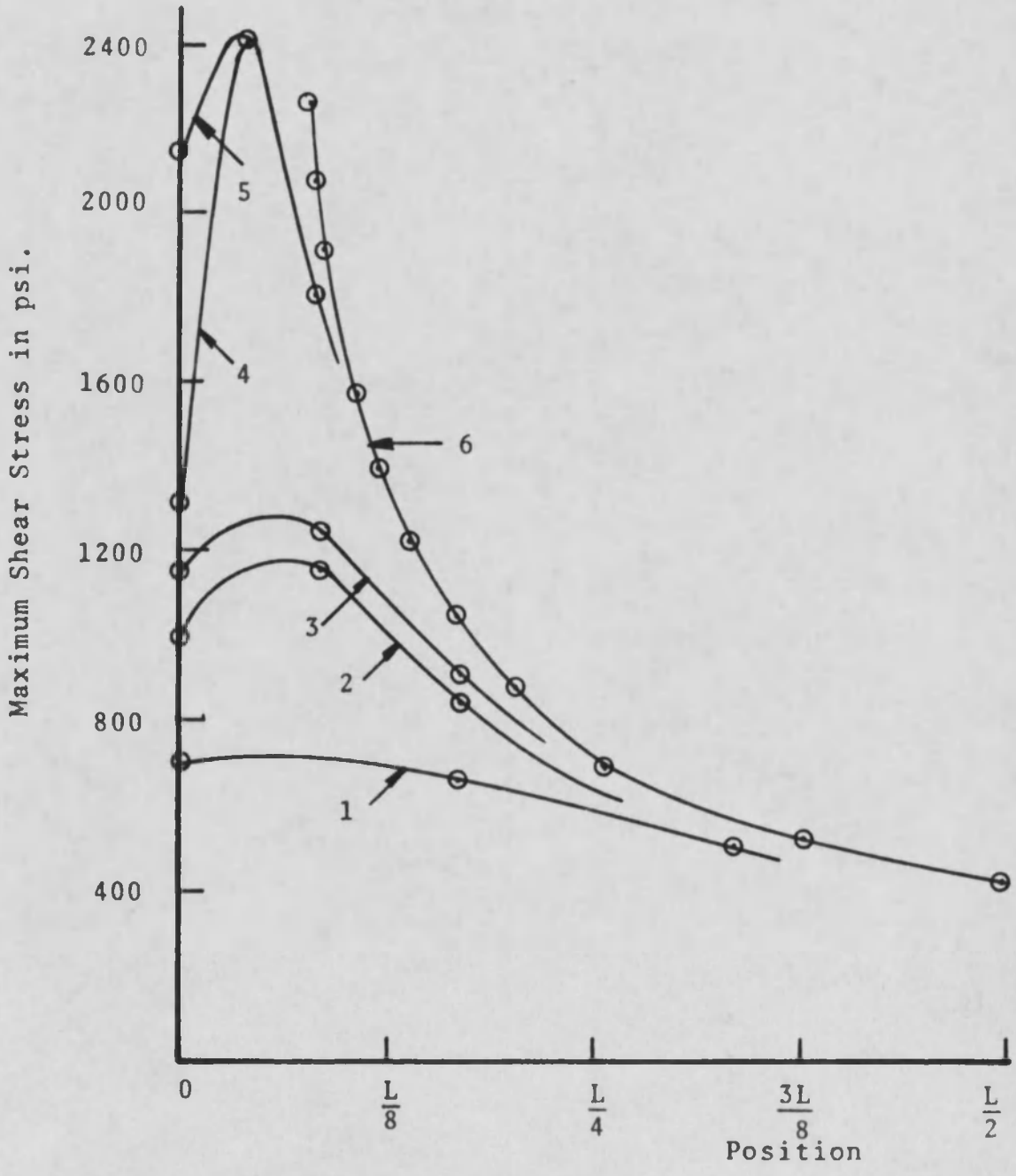

Figure 6

Maximum Shear Stress as a Function of Position from the Load Point to the Middle of the Plate

Figure 7

Maximum Shear Stress as a Function of Position

from the Middle of the Plate to the Clamped Edge

Curve 1 -- the fine mesh solution
Curve 2 -- the photoelastic solution

The photoelastic solution is shown in its entirety as well as the photograph could be read. For clarity, the other four numerical solutions are omitted. All portions of the omitted curves lie within 60 psi. of the photoelastic solution. On the abscissa, the zero point is the middle of the plate and L/2 is the clamped edge.

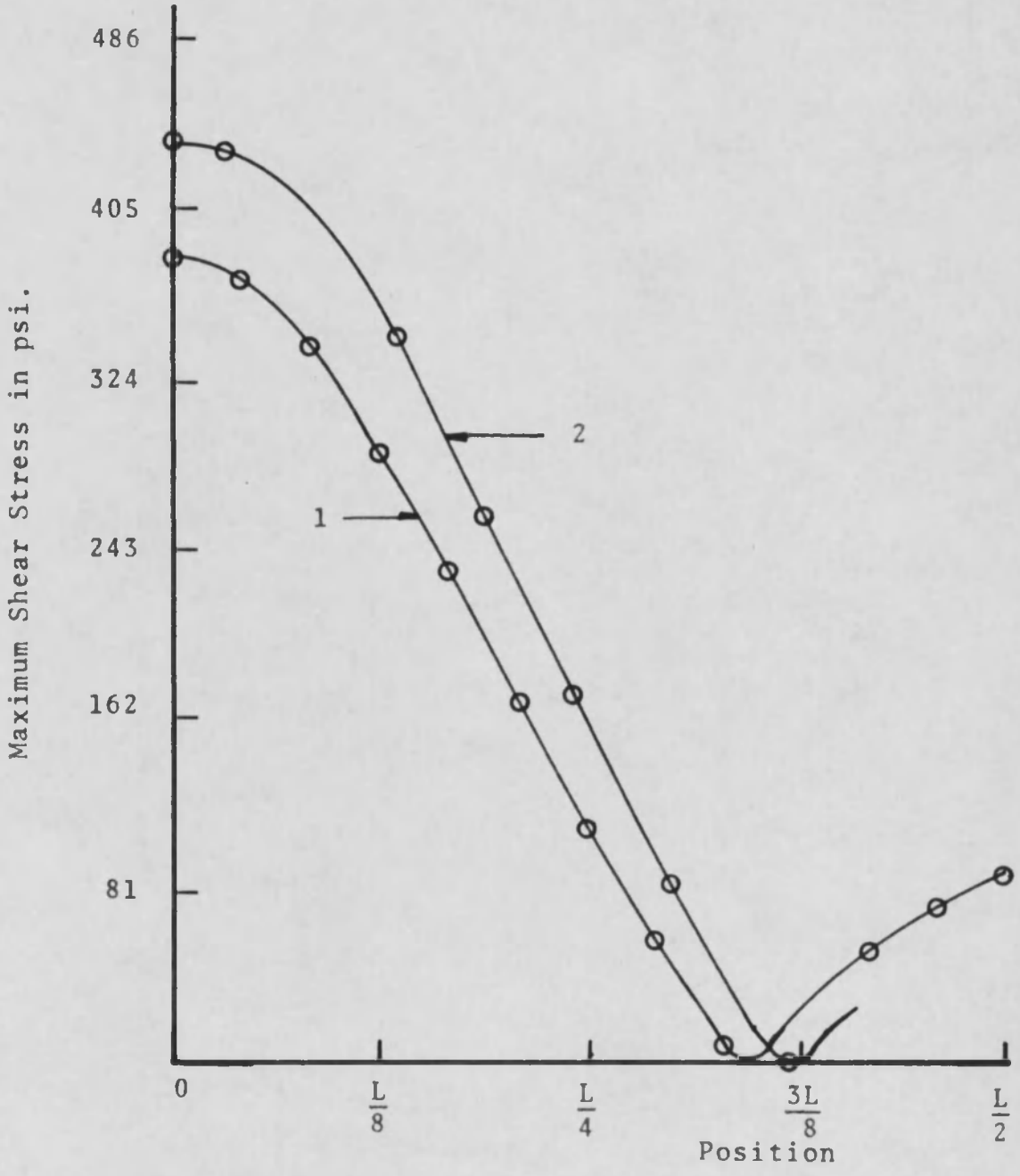

Figure 7

Maximum Shear Stress as a Function of Position from the Middle of the Plate to the Clamped Edge

methods, the regions of the plate with the largest errors are the regions where the displacements are the smallest. Because of these two opposing considerations, it is practically impossible to determine which parts of the numerical solutions should contain the least error. So it is necessary to consider both regions of high stress and regions of low stress when comparing the finite-difference solutions with the photoelastic solution.

Considering first the numerical solutions, Figure 6 shows that the coarse mesh, coarse graded mesh, and middle-sized mesh solutions failed to detect the initial maximum value of the shear stress in the vicinity of the applied load. For these solutions, the mesh size was too large to model the load properly. In a finite-difference solution, a point load must be replaced by a statically equivalent load distributed over a length of the edge of the plate equal to one mesh length, h. This reduces the maximum value of shear stress in the vicinity of the load. However, by Saint Venant's Principle, the stress distribution should be the same a sufficient distance away from the load. Figure 6 shows that the sufficient distance for these three solutions is two mesh lengths. Two mesh lengths away from the load the coarse mesh, the coarse graded mesh, and the middle-sized mesh solutions appear to be good approximations of the photoelastic solution.

The fine graded mesh and the fine mesh solutions also contain a large error in the vicinity of the applied load. However, due to the smaller mesh size, they more closely approximate the steep gradient in the shear stress in the vicinity of the load. Again, these solutions are good approximations to the photoelastic solution at any point in the plate at least two mesh lengths away from the load point. It should be mentioned here that, due to the local lens, the photoelastic results are of questionable accuracy within two fine mesh lengths of the applied load.

Photoelastic Solution as a Measure of the Accuracy of the Numerical Solutions

From the curves in Figure 6 and Figure 7, the numerical solutions are all within 160 psi. of the photoelastic solution for all points at least two mesh lengths away from the applied load. The coarse mesh, coarse graded mesh, and middle-sized mesh solutions must be regarded as poor approximations to the photoelastic solution due to their inability to detect the large stress gradient in the vicinity of the load.

The fine graded mesh and the fine mesh solutions have a small enough grid spacing to detect the initial steep gradient in the maximum shear stress. These two solutions are within 120 psi. of the photoelastic solution

for an applied load of 405 pounds. The largest maximum shear stress in the plate is approximately 2400 psi. So the error in these two numerical solutions as compared to the photoelastic solution is 5 per cent of the largest maximum shear stress. Of course, in the regions of low maximum shear stress, the percentage error is large, but the region of high shear stress is of greatest interest, and here the percentage error is low. From economic considerations, it is difficult to choose between the fine graded mesh and the fine mesh solutions, since they both ran eight minutes on the IBM 7072 computer.

The fine graded mesh solution was designed to yield results comparable to the fine mesh solution in the vicinity of the load while saving computer time by using fewer nodal points and therefore having to solve a smaller set of equations. However, the computer program used for the graded mesh solution was written in a form which minimized programming difficulties but not computation time. Had computation time been the prime consideration, the fine graded mesh would have yielded a solution in approximately 30 per cent less time than the fine mesh. This estimate is based upon the relative convergence rates of the middle-sized mesh and coarse graded mesh solutions as listed in Table 1, and applies only to the specific problem proposed in this thesis.

Therefore, considering economy and accuracy, the fine graded mesh solution provides the best approximation to the photoelastic solution for the problem proposed in this thesis.

Conclusions

The study undertaken in this thesis leads to three conclusions.

First, the finite-difference solution of Navier's Equations yields a good approximate solution to a mixed boundary-value problem in plane elasticity. This, of course, presupposes that a sufficiently small mesh is used.

Second, Faddeeva's acceleration scheme can reduce convergence time by one half for an iterative solution of a system of linear algebraic equations. Perhaps with a different system of equations, even better results could be obtained.

Third, a variable mesh procedure should be employed in order to model an applied load more accurately or to detect regions where the displacement gradient is large. This will increase the accuracy of the finite-difference solution in the regions of greatest interest while keeping the computation time to a minimum.

Proposal for Future Investigation

The results of this thesis indicate the desirability of further investigation into Faddeeva's acceleration scheme. Faddeeva's scheme was applied to three sets of equations in this thesis and increased their convergence rates by 50 per cent. This is a substantial saving in computer time. However, before any broad statement concerning Faddeeva's scheme can be made, it must be tested on many different sets of equations.

One important aspect of Faddeeva's acceleration scheme is that the slower the convergence of the iterative solution, the more effective the acceleration scheme. This is due to the fact that the dominant eigenvalue of the iteration matrix, which is a measure of the rate of convergence, is used to accelerate the convergence. So any future investigation should include a few sets of equations with a relatively fast rate of convergence and a larger number with a relatively slow rate of convergence. In this way, it would be possible to measure, over a large range, the percentage of computer time saved using Faddeeva's acceleration scheme.

Professor Richmond C. Neff of the University of Arizona has presented in his lectures an acceleration scheme which is, in effect, a higher order form of Faddeeva's scheme. This higher order acceleration scheme

consists in extracting the first two or three dominant eigenvalues and using these to accelerate the rate of convergence. The higher order method could be of significant value whenever the first two or three dominant eigenvalues have approximately the same magnitude. This scheme was not used in this thesis, but due to the success of Faddeeva's scheme, any future investigation should give the higher order scheme serious consideration.

APPENDIX

The following is the computer program used to solve the flat plate problem using the fine mesh. The program is written in Fortran II language and was run on the IBM 7072 computer at the University of Arizona.

```
C       GAUSS-SEIDEL ITERATION WITH AN ACCELERATION SCHEME
C       BY FADDEEVA
        DIMENSION UOLD(15,15),VOLD(15,15),U(15,15),V(15,15),
       1SUMX(900),ANORM(899),EIG(898),TSUMX(900),ANORT(899),
       2T11(15,15),T22(15,15),T12(15,15),TMAX(15,15)
        READ 600,NI,NJ,MERR
        READ 601,AMERR,CONST,ALAM,AMU,P
        READ 601,SIZE
        K=1
        M=0
        MCNT=0
        NU=NI-1
        NV=NJ-1
        DO 1 I=1,NI
        DO 1 J=1,NJ
        U(I,J)=0.0
      1 V(I,J)=0.0
     10 M=M+1
        MCNT=MCNT+1
C       TEST FOR NUMBER OF ITERATIONS
        IF(M-MERR)11,11,500
     11 DO 12 I=1,NU
        DO 12 J=2,NV
        UOLD(I,J)=U(I,J)
     12 VOLD(I,J)=V(I,J)
        DO 90 J=2,NV
        DO 89 I=1,NU
        DO 13 L=1,NU
C       SYMMETRY CONDITIONS
        U(L,1)=-U(L,3)
     13 V(L,1)=V(L,3)
        DO 14 L=2,NV
        V(15,L)=-V(13,L)
     14 U(15,L)=U(13,L)
        IF(I-1)15,25,15
```

```
   15 IF(J-2)16,26,16
   16 IF(I-14)17,27,17
   17 IF(I-2)24,18,24
   18 IF(J-13)24,28,24
C       WORKING EQUATIONS
   24 U(I,J)=((1.0+CONST)*(U(I,J+1)+U(I,J-1))+(CONST/4.0)*
     1(VI-1,J+1)-V(I+1,J+1)-V(I-1,J-1)+V(I+1,J-1))
     2+U(I-1,J)+U(I+1,J))/(2.0*(2.0+CONST))
   33 V(I,J)=((1.0+CONST)*(V(I-1,J)+V(I+1,J))+(CONST/4.0)*
     1(U(I-1,J+1)-U(I-1,J-1)-U(I+1,J+1)+U(I+1,J-1))
     2+V(I,J+1)+V(I,J-1))/(2.0*(2.0+CONST))
      GO TO 89
   25 U(I,J)=U(I+2,J)+V(I+1,J-1)-V(I+1,J+1)
      IF(J-2)31,32,31
   31 V(I,J)=(-ALAM*(U(I+1,J+1)-U(I+1,J-1)))/(2.0*(AMU+
     1ALAM))+V(I+2,J)
      GO TO 89
   32 V(I,J)=(-P*((ALAM+2.0*AMU)/AMU)-ALAM*(U(I+1,J+1)-
     1U(I+1,J-1)))/(2.0*(AMU+ALAM))+V(I+2,J)
      GO TO 89
   26 IF(I-14)33,89,33
   27 U(I,J)=((1.0+CONST)*(U(I,J+1)+U(I,J-1))+(CONST/4.0)*
     1(V(I-1,J+1)-V(I+1,J+1)-V(I-1,J-1)+V(I+1,J-1))
     2+U(I-1,J)+U(I+1,J))/(2.0*(2.0+CONST)
      GO TO 89
   28 U(I,J)=((1.0+CONST)*(U(I,J+1)+U(I,J-1))+(CONST/4.0)*
     1(V(I+2,J+1)-V(I+2,J-1)-4.0*V(I+1,J+1)+4.0*V(I+1,J-1)
     2+3.0*V(I,J+1)-3.0*V(I,J-1))+U(I-1,J)+U(I+1,J))/(2.0*
     3(2.0+CONST))
      V(I,J)=((1.0+CONST)*(V(I-1,J)+V(I+1,K))+(CONST/4.0)*
     1(U(I+2,J+L)-U(I+2,J-1)-4.0*U(I+1,J+1)+4.0*U(I+1,J-1)
     2+3.0*U(I,J+1)-3.0*U(I,J-1))+V(I,J+1)+V(I,J-1))/(2.0*
     3(2.0+CONST))
      GO TO 89
   89 CONTINUE
   90 CONTINUE
   39 SUMX(M)=0.0
      TSUMX(M)=0.0
      DO 40 I=1,NU
      DO 40 J-2,NV
      TSUMS(M)=TSUMX(M)+ABSF(U(I,J))+ABSF(V(I,J))
   40 SUMX(M)=SUMX(M)+U(I,J)+V(I,J)
      IF(M-1)10,10,41
   41 ANORM(M-1)=SUMX(M)-SUMX(M-1)
      ANORT(M-1)=ABSF(TSUMX(M)-TSUMX(M-1))
      IF(M-2)10,10,50
C       TEST FOR CONVERGENCE OF SYSTEM
   50 TEST=ABSF(ANORT(M)-ANORT(M-1))
      IF(TEST-.001*ANORT(M))500,500,51
   51 IF(K-1)52,52,70
```

```
     52 EIG(M-2)=(ANORM(M-1))/(ANORM(M-2))
        IF(M-3)10,10,53
C       TEST FOR CONVERGENCE OF EIGENVALUE
     53 CH=ABSF(EIG(M-2)-EIG(M-3))
        IF(CH-AMERR)60,60,10
     60 K=2
        AMBDA=EIG(M-2)
        MIT = M
        MCNT=MIT
C       TEST FOR APPLICATION OF ACCELERATION SCHEME
     70 IF(MCNT-MIT)10,71,10
C       ACCELERATION SCHEME
     71 DO 72 I=1,NU
        DO 72 J=2,NV
        U(I,J)=UOLD(I,J)+(U(I,J)-UOLD(I,J))/(1.0-AMBDA)
     72 V(I,J)=VOLD(I,J)+(V(I,J)-VOLD(I,J))/(1.0-AMBDA)
        MCNT=0
        GO TO 10
    500 PRINT 701,M
    701 FORMAT (24HONUMBER OF ITERATIONS = I3)
        PRINT 702,AMBDA
    702 FORMAT(23HODOMINANT EIGENVALUE = 1F10.7)
        PRINT 703,MIT
    703 FORMAT (25HOACCELERATION INTERVAL = I3)
        PRINT 704
    704 FORMAT (25HOHORIZONTAL DISPLACEMENTS/)
        PRINT 700,((U(I,J),J=2,NV),I=1,NU)
        PRINT 705
    705 FORMAT (23HOVERTICAL DISPLACEMENTS/)
        PRINT 700, ((V(I,J),J=2,NV),I=1,NU)
    700 FORMAT (6E19.7)
    600 FORMAT (8I10)
    601 FORMAT (8F10.0)
C       CALCULATE STRESSES
        CA=(2.0*AMU*(ALAM+AMU))/(ALAM+(2.0*AMU))
        CB=(AMU*ALAM)/(ALAM+(2.0*AMU))
        SZ=.5*SIZE*AMU
        DO 901 I=2,NU
        DO 901 J=2,NV
        T11(I,J)=SIZE*(CA*(U(I,J+1)-U(I,J-1))+CB*(V(I-1,J)-
       1V(I+1,J)))
        T22(I,J)=SIZE*(CA*(V(I-1,J)-V(I+1,J))+CB*(U(I,J+1)-
       1U(I,J-1)))
    901 DO 902 I=3,NU
        J=NJ
        T11(I,J)=SIZE*(CA*(U(I,J-2)-(4.0*U(I,J-1))+(3.0*
       1U(I,J)))+CB*(V(I-1,J)-V(I+1,J)))
        T22(I,J)=SIZE*(CA*(V(I-1,J)-V(I+1,J))+CB*(U(I,J-2)-
       1(4.0*U(I,J-1))+(3.0*U(I,J))))
```

```
902 T12(I,J)=SZ*(U(I-1,J)-U(I+1,J)+V(I,J-2)-(4.0*
   1V(I,J-1))+(3.0*V(I,J)))
    T11(2,NJ)=SIZE*(CA*(U(2,NJ-2)-(4.0*U(2,NJ-1))+(3.0*
   1U(2,NJ)))+CB*(V(4,NJ)-(4.0*V(3,NJ))+(3.0*V(2,NJ))))
    T22(2,NJ)=SIZE*(CA*(V(4,NJ)-(4.0*V(3,NJ))+(3.0*V(2,
   1NJ)))+CB*(U(2,NJ-2)-4.0*U(2,NJ-1))+(3.0*U(2,NJ))))
    T12(2,NJ)=SZ*(U(4,NJ)-(4.0*U(3,NJ))+(3.0*U(2,NJ))
   1+V(2,NJ-2)-(4.0*V(2,NJ-1))+(3.0*V(2,NJ)))
    PRINT 907
    PRINT 905,((T11(I,J),J-2,NJ),I=2,NU)
    PRINT 906
    PRINT 905,((T22(I,J),J=2,NJ),I=2,NJ)
    PRINT 908
    PRINT 905,((T12,(I,J),J=2,NJ),I=2,NU)
905 FORMAT (6E19.7)
906 FORMAT (23HOVERTICAL NORMAL STRESS/)
907 FORMAT (25HOHORIZONTAL NORMAL STRESS/)
908 FORMAT (13HOSHEAR STRESS/)
    DO 200 I=2,NU
    DO 200 J=2,NJ
200 TMAX(I,J)=SQRTF((.5*(T11(I,J)-T22(I,J)))**2+(T12
   1(I,J))**2)
    PRINT 909
909 FORMAT (21HOMAXIMUM SHEAR STRESS/)
    PRINT 905,((TMAX(I,J),J=2,NJ),I=2,NU)
    STOP
    END
```

REFERENCES

Allen, D. N. de G., Relaxation Methods in Engineering and Science, McGraw-Hill Book Company, Inc., New York, 1954.

Boresi, Arthur P., Elasticity in Engineering Mechanics, Prentice-Hall, Inc., Englewood Cliffs, New Jersey, 1965.

Faddeeva, V. N., Computational Methods of Linear Algebra, Dover Publications, Inc., New York, 1959.

Griffin, D. S. and R. S. Varga, "Numerical Solution of Plane Elasticity Problems," Journal of the Society for Industrial and Applied Mathematics, Vol. 11, No. 4, December, 1963, pp. 1046-62.

Jessop, H. T. and F. C. Harris, Photoelasticity: Principle and Methods, Dover Publications, Inc., New York, 1950.

Lee, George Hamor, An Introduction to Experimental Stress Analysis, John Wiley & Sons, Inc., New York, 1950.

Salvadori, Mario G. and Melvin L. Baron, Numerical Methods in Engineering, 2nd Edition, Prentice-Hall, Inc., Englewood Cliffs, New Jersey, 1961.

Scarborough, James B., Numerical Mathematical Analysis, 4th Edition, The Johns Hopkins Press, Baltimore, 1958.

Sokolnikoff, I. S., Mathematical Theory of Elasticity, 2nd Edition, McGraw-Hill Book Company, Inc., New York, 1956.